

# Identification of novel hyper- or hypomethylated CpG sites and genes associated with atherosclerotic plaque using an epigenome-wide association study

YOSHIJI YAMADA<sup>1,2</sup>, HIDEKI HORIBE<sup>3</sup>, MITSUTOSHI OGURI<sup>1,4</sup>, JUN SAKUMA<sup>2,5,6</sup>,  
ICHIRO TAKEUCHI<sup>2,6,7</sup>, YOSHIKI YASUKOCHI<sup>1,2</sup>, KIMIHIKO KATO<sup>1,8</sup> and MOTOJI SAWABE<sup>9</sup>

<sup>1</sup>Department of Human Functional Genomics, Advanced Science Research Promotion Center, Mie University, Tsu 514-8507;

<sup>2</sup>CREST, Japan Science and Technology Agency, Kawaguchi 332-0012; <sup>3</sup>Department of Cardiovascular Medicine,

Gifu Prefectural Tajimi Hospital, Tajimi 507-8522; <sup>4</sup>Department of Cardiology, Kasugai Municipal Hospital,

Kasugai 486-8510; <sup>5</sup>Computer Science Department, College of Information Science, University of Tsukuba,

Tsukuba 305-8573; <sup>6</sup>RIKEN Center for Advanced Intelligence Project, Tokyo 103-0027;

<sup>7</sup>Department of Computer Science, Nagoya Institute of Technology, Nagoya 466-8555;

<sup>8</sup>Department of Internal Medicine, Meitoh Hospital, Nagoya 465-0025;

<sup>9</sup>Section of Molecular Pathology, Graduate School of Health Care Sciences,

Tokyo Medical and Dental University, Tokyo 113-8510, Japan

Received October 11, 2017; Accepted January 23, 2018

DOI: 10.3892/ijmm.2018.3453

**Abstract.** DNA methylation is an important epigenetic modification that has been implicated in the pathogenesis of atherosclerosis. Although previous studies have identified various CpG sites and genes whose methylation is associated with atherosclerosis in populations with European or Mexican ancestry, the genome-wide pattern of DNA methylation in the atherosclerotic human aorta is yet to be elucidated in Japanese individuals. In the present study, a genome-wide analysis of DNA methylation at ~853,000 CpG sites was performed using 128 postmortem aortic intima specimens obtained from 64 Japanese patients. To avoid the effects of interindividual variation, intraindividual paired comparisons were performed between atheromatous plaque lesions and corresponding plaque-free tissue for each patient. Bisulfite-modified genomic DNA was analyzed using a specific microarray for DNA methylation. DNA methylation at each CpG site was calculated as the  $\beta$  value, where  $\beta = (\text{intensity of the methylated allele})/(\text{intensity of the methylated allele} + \text{intensity of the unmethylated allele} + 100)$ . Bonferroni's correction for statistical significance of association was applied to compensate for multiple comparisons. The methylation of 2,679 CpG

sites differed significantly ( $P < 5.86 \times 10^{-8}$ ) between atheromatous plaque lesions and the corresponding plaque-free intima, with 2,272 and 407 CpG sites in atheromatous plaques being hyper- or hypomethylated, respectively. A total of 5 hypermethylated CpG sites in atheromatous plaques were demonstrated to have a difference in  $\beta$  value of  $>0.15$  (plaque lesion-plaque-free intima) and 11 had a  $\beta$  ratio of  $>1.50$  (plaque/plaque-free intima). A further 15 and 17 hypomethylated CpG sites in atheromatous plaques were observed to have a difference in  $\beta$  value of  $<-0.15$  or a  $\beta$  ratio of  $<0.67$ , respectively. According to these limits, a total of 16 novel genes that were significantly hyper- or hypomethylated in atheromatous plaque lesions compared with the plaque-free intima were identified in the present study. The results of the present study suggest that the methylation of these genes may contribute to the pathogenesis of atherosclerosis in the Japanese population.

## Introduction

Atherosclerosis is a chronic inflammatory vascular disease characterized by infiltration of lipid particles into the arterial wall, leading to inflammatory responses accompanied by endothelial cell dysfunction and recruitment of inflammatory and immune cells (1). Previous studies have reported that epigenetic mechanisms may be associated with the pathogenesis of atherosclerosis and may account for some of the missing heritability in atherosclerotic cardiovascular disease (2,3). Epigenetic control of transcription results in a heritable change in gene expression without a change in DNA sequence. DNA methylation and post-translational modifications of histone tails, including lysine methylation and acetylation, are the most common mechanisms that cause changes in DNA accessibility (3).

*Correspondence to:* Professor Yoshiji Yamada, Department of Human Functional Genomics, Advanced Science Research Promotion Center, Mie University, 1577 Kurima-machiya, Tsu, Mie 514-8507, Japan  
E-mail: yamada@gene.mie-u.ac.jp

**Key words:** atherosclerosis, cardiovascular disease, DNA methylation, epigenetics, epigenome-wide association study

DNA methylation is a vital epigenetic modification that has been implicated in the pathogenesis of a number of common complex diseases, including atherosclerosis and cardiovascular disease (4-12). DNA methylation serves a role in a variety of cellular processes (5,13), is affected by environmental factors and is influenced by age, sex and genetic variants (4,6). As such, elucidating the differences in DNA methylation patterns between atherosclerotic plaque lesions and plaque-free intima tissue may provide an insight into the underlying molecular mechanisms of atherosclerotic cardiovascular disease. Although previous analyses of DNA methylation have identified various CpG sites and genes associated with atherosclerosis in European-ancestry (14-17) or Mexican (18) populations, the pattern of DNA methylation in the atherosclerotic human aorta at the genome-wide level has remained relatively uncharacterized in Japanese individuals.

A previous study examined DNA methylation at ~450,000 CpG sites (Human Methylation 450 BeadChip; Illumina, Inc., San Diego, CA, USA) in 48 human aortic intima specimens obtained from 24 autopsy cases (19); it was demonstrated that DNA methylation was significantly ( $P < 1.03 \times 10^{-7}$ ) increased at 30 CpG sites and reduced at 15 CpG sites in atheromatous plaque tissues compared with plaque-free intima (19). In the present study, to further assess the association between DNA methylation and the development of atherosclerosis, a genome-wide analysis of DNA methylation at ~853,000 CpG sites (Infinium MethylationEPIC BeadChip) was performed in 128 human aortic intima specimens obtained from 64 autopsy cases. Compared with the Human Methylation 450 BeadChip array, the newly developed Infinium MethylationEPIC BeadChip array is a more reliable tool for comprehensive DNA methylation analyses (20). A total of 16 significantly hyper- or hypomethylated novel genes in atheromatous plaque lesions were identified.

## Materials and methods

**Study specimens.** Characteristics of the 64 deceased patients from whom tissues were harvested for use in the present study are presented in Table I. Inter-individual variation in DNA methylation was detected for the same cell and tissue type of unrelated individuals (21,22). To avoid the effects of such variation, intra-individual paired comparisons of DNA methylation were performed between atheromatous plaque lesions and corresponding plaque-free intima. A total of 128 postmortem specimens of the aortic intima were obtained from 64 deceased Japanese patients for analysis. The specimens were collected specifically for this study in participating hospitals (Gifu Prefectural Tajimi Hospital, Tajimi; Japanese Red Cross Nagoya First Hospital, Nagoya; Kasugai Municipal Hospital, Kasugai; Tokyo Metropolitan Geriatric Hospital, Tokyo, Japan) between August 2012 and August 2017. A total of 48 of these specimens obtained from 24 subjects were also analyzed in a previous study (19).

**Immunohistochemical analysis of atheromatous plaque lesions and plaque-free intima.** Specimens of atheromatous plaque lesions and plaque-free intima were subjected to immunohistochemical analysis as described previously (19). Formalin (20%)-fixed (6 h at room temperature) and paraffin-embedded

Table I. Patient characteristics (n=64).

| Characteristic   | Value                      |
|--|----------------------------|
| Mean age (years) $\pm$ SD (range)                          | 75.8 $\pm$ 12.9 (41-95)    |
| Sex (male/female, %)                                       | 73.4/26.6                  |
| Mean body mass index (kg/m <sup>2</sup> ) $\pm$ SD (range) | 19.8 $\pm$ 4.3 (12.2-32.2) |
| Current or former smoker (%)                               | 57.5                       |
| Hypertension (%)   | 40.6                       |
| Diabetes mellitus (%)                                      | 20.3                       |
| Dyslipidemia (%)   | 9.4                        |
| Chronic kidney disease (%)                                 | 32.8                       |
| Myocardial infarction (%)                                  | 21.9                       |
| Ischemic stroke (%)  | 9.4                        |
| Cause of death (n)   |                            |
| Pneumonia  | 13                         |
| Myocardial infarction                                      | 12                         |
| Dissecting aortic aneurysm                                 | 4                          |
| Amyloidosis  | 2                          |
| Dilated cardiomyopathy                                     | 2                          |
| Hypertrophic cardiomyopathy                                | 2                          |
| Interstitial pneumonia                                     | 2                          |
| Lung cancer  | 2                          |
| Necrotizing enterocolitis                                  | 2                          |
| Amyotrophic lateral sclerosis                              | 1                          |
| Arrhythmogenic right ventricular cardiomyopathy            | 1                          |
| Aspergillosis  | 1                          |
| Bacterial meningitis                                       | 1                          |
| Cardiac sarcoidosis  | 1                          |
| Chronic obstructive pulmonary disease                      | 1                          |
| Embolic stroke   | 1                          |
| Gastric cancer   | 1                          |
| Heatstroke   | 1                          |
| Huntingdon's disease                                       | 1                          |
| Intestinal obstruction                                     | 1                          |
| Ischemic heart disease                                     | 1                          |
| Malignant mesothelioma                                     | 1                          |
| Malnutrition   | 1                          |
| Multiple myeloma   | 1                          |
| Parkinson's disease  | 1                          |
| Primary biliary cirrhosis                                  | 1                          |
| Pulmonary hypertension                                     | 1                          |
| Relapsing polychondritis                                   | 1                          |
| Renal failure  | 1                          |
| Superior mesenteric artery thrombosis                      | 1                          |
| Traumatic lung contusion                                   | 1                          |
| Valvular heart disease                                     | 1                          |

SD, standard deviation.

sections (3  $\mu\text{m}$ ) were deparaffinized, hydrated, immersed in 0.01 mol/l citrate buffer (pH 6.0), and heated for 10 min in a pressure cooker. Endogenous peroxidase was blocked with 3% hydrogen peroxide for 5 min at room temperature and sections were incubated for 30 min at room temperature with mouse monoclonal antibodies against human  $\alpha$ -smooth muscle actin (1:100; M0851; Dako; Agilent Technologies, Inc., Santa Clara, CA, USA), CD68 (1:100; N1576; Dako; Agilent Technologies, Inc.) and CD45 (1:100; 722071; Nichirei Bioscience, Inc., Tokyo, Japan). Proteinase K (0.1%) pre-treatment (5 min at room temperature) was used for CD68 and CD45. Sections were subsequently incubated for 30 min at room temperature with horseradish peroxidase (HRP)-conjugated goat polyclonal antibody to rabbit and mouse immunoglobulin (1:100; K5007; Dako; Agilent Technologies, Inc.). Sections were stained with diaminobenzidine for 10 min at room temperature (ChemMate Envision/HRP kit; K5007; Dako; Agilent Technologies, Inc.).

The present study was approved by the Committees on the Ethics of Human Research of: Mie University Graduate School of Medicine, Tsu; Tokyo Metropolitan Institute of Gerontology, Tokyo; Japanese Red Cross Nagoya First Hospital, Nagoya; Gifu Prefectural Tajimi Hospital, Tajimi; and Kasugai Municipal Hospital, Kasugai (all Japan). Written informed consent was obtained from the families of the deceased patients.

**Genome-wide analysis of DNA methylation.** The intima tissue samples were frozen at  $-80^{\circ}\text{C}$  immediately following dissection from the aorta. The finely minced (cut to  $\sim 1\text{ mm}^3$  with a surgical blade) tissue was subsequently mixed with 250  $\mu\text{l}$  phenol-chloroform and centrifuged at  $12,000 \times g$  for 5 min at room temperature. The upper aqueous phase was collected for the precipitation of genomic DNA and 100% ethanol containing 0.3 mol/l sodium acetate was added and incubated at  $-30^{\circ}\text{C}$  for 30 min. The mixture was then centrifuged at  $12,000 \times g$  for 20 min at  $4^{\circ}\text{C}$  and the DNA pellet was dissolved in Tris-EDTA buffer (pH 7.4; Takara Bio, Inc., Otsu, Japan). Bisulfite conversion of genomic DNA was performed using an EZ DNA Methylation kit (Zymo Research Corp., Irvine, CA, USA).

The bisulfite-modified genomic DNA was analyzed for DNA methylation with a DNA methylation-specific microarray (Infinium MethylationEPIC BeadChip, Illumina, Inc.) that included 853,307 CpG sites distributed throughout the entire genome. A total of 439,562 (91.1%) of these sites were assessed in a previous study (19) using the Human Methylation 450 BeadChip. Furthermore, 413,745 additional CpG sites, including 333,265 located in enhancer regions, were identified by the Encyclopedia of DNA elements (23) and FANTOM5 (24) projects. The Infinium Methylation EPIC BeadChip microarray also interrogates 2,880 CNG (C, cytosine; N, any nucleotide; G, guanine) sites (20).

Methylation at CpG sites in genomic DNA isolated from atheromatous plaque lesions or plaque-free intima was assessed using a GenomeStudio Methylation Module (Illumina, Inc.). Call rate values for the 128 specimens were all  $>99.3\%$ , with a mean value of  $99.7\%$ . The DNA methylation level at each CpG site was calculated as the  $\beta$  value, where  $\beta = (\text{intensity of the methylated allele})/(\text{intensity of the methylated allele} + \text{intensity of the unmethylated allele} + 100)$  (25).

**Statistical analysis.** The levels of DNA methylation at 853,307 CpG sites ( $\beta$  values) were compared between atheromatous plaque lesions and plaque-free intima using the unpaired Student's t-test. To compensate for multiple comparisons, Bonferroni's correction for the statistical significance of associations was used. The significance level was thus  $P < 5.86 \times 10^{-8}$  ( $0.05/853,307$ ) for the genome-wide analysis of DNA methylation. Statistical tests were performed using JMP Genomics 6.0 software (SAS Institute, Inc., Cary, NC, USA).

**Analysis of public databases.** The potential association between CpG sites and genes identified in the present study with atherosclerosis was assessed by searching public databases between January 2007 and October 2017 [Google Scholar (<http://scholar.google.co.jp>); PubMed (National Center for Biotechnology Information, Bethesda, MD, USA; <https://www.ncbi.nlm.nih.gov/pubmed>), GWAS Catalog (National Human Genome Research Institute, Bethesda, MD, USA and European Bioinformatics Institute, Hinxton, UK; <http://www.ebi.ac.uk/gwas>) and GWAS Central (<http://www.gwascentral.org>)] for previously associated phenotypes. Genome-wide analyses of DNA methylation or genome-wide association studies for atherosclerosis or cardiovascular disease were included in the results. DNA methylation analyses or association studies of candidate genes were excluded.

## Results

**Study specimens.** In the present study, the methylation status of 853,307 CpG sites of genomic DNA purified from atheromatous plaque lesions and corresponding plaque-free intima were compared. Manhattan and volcano plots for the genome-wide analysis of differences in methylation status at these sites are presented in Figs. 1 and 2, respectively. Following Bonferroni's correction, the methylation of 2,679 CpG sites was revealed to differ significantly ( $P < 5.86 \times 10^{-8}$ ) between atheromatous plaque lesions and corresponding plaque-free intima. The 50 CpG sites with the lowest P-values ( $P \leq 3.48 \times 10^{-12}$ ) are presented in Table II; to the best of our knowledge, none of these sites have previously been reported to be associated with atherosclerosis.

**Genome-wide analysis of gene methylation.** Of the 2,679 CpG sites significantly associated with atherosclerosis, 2,272 and 407 sites were hyper- or hypomethylated, respectively, in atheromatous plaque lesions compared with plaque-free intima. Among the 2,272 CpG sites that were hypermethylated in atheromatous plaque lesions, 5 had a  $\beta$  value difference (plaque lesion-plaque-free intima)  $>0.15$  (Table III) and 11 had a  $\beta$  ratio (plaque lesion/plaque-free intima)  $>1.50$  (Table IV). Among these CpG sites, cg15648389 of homeobox (*HOX*) C4 (15), cg17466857 of *HOXA11-HOXA11-AS* (14,15), cg15700739 of *HOXC4/HOXC5* (17) and cg02384661 of *HOXC11* (15) have previously been demonstrated to be associated with atherosclerosis.

Among the 407 CpG sites hypomethylated in atheromatous plaque lesions, 15 were observed to have a  $\beta$  value difference  $<0.15$  (Table V) and 17 sites had a  $\beta$  ratio  $<0.67$  (Table VI). Of these CpG sites, cg03217995 of *HOXA9* (15) was previously reported to be associated with atherosclerosis.

Table II. A total of 50 CpG sites with the lowest P-values ( $P \leq 3.48 \times 10^{-12}$ ) for the comparison of methylation status ( $\beta$  values) between atheromatous plaque lesions and plaque-free intima by a genome-wide analysis of DNA methylation.

| CpG        | Chromosome:<br>position | Gene  | Methylation<br>site | Mean $\beta$ value<br>(plaque) | Mean $\beta$ value<br>(plaque-free) | $\beta$ ratio (plaque/<br>plaque-free) | P-value                |
|------------|-------------------------|---|---------------------|--------------------------------|-------------------------------------|--|------------------------|
| cg06792393 | 5:139242953             | <i>NRG2</i>   | Body                | 0.7906                         | 0.6985                              | 1.13                                   | $1.11 \times 10^{-16}$ |
| cg19517104 | 7:134204895             |   |                     | 0.8458                         | 0.7535                              | 1.12                                   | $5.60 \times 10^{-15}$ |
| cg02580923 | 12:117470541            |   |                     | 0.4173                         | 0.5093                              | 0.82                                   | $9.21 \times 10^{-15}$ |
| cg15374435 | 13:80911692             | <i>SPRY2</i>  | Body                | 0.7301                         | 0.5885                              | 1.24                                   | $1.42 \times 10^{-14}$ |
| cg15796536 | 5:140873082             | <i>PCDHGA8</i>  | Body                | 0.8437                         | 0.7766                              | 1.09                                   | $1.82 \times 10^{-14}$ |
| cg06827792 | 7:36723794              | <i>AOAH</i>   | Body                | 0.8015                         | 0.7180                              | 1.12                                   | $1.92 \times 10^{-14}$ |
| cg06996940 | 15:28197405             | <i>OCA2</i>   | Body                | 0.8065                         | 0.7492                              | 1.08                                   | $3.82 \times 10^{-14}$ |
| cg25506501 | 3:59521337              |   |                     | 0.7693                         | 0.6500                              | 1.18                                   | $5.56 \times 10^{-14}$ |
| cg22055728 | 7:27205658              | <i>HOXA9</i>  | TSS1500             | 0.1162                         | 0.2026                              | 0.57                                   | $7.80 \times 10^{-14}$ |
| cg15542608 | 6:12827379              | <i>PHACTR1</i>  | Body                | 0.8312                         | 0.7371                              | 1.13                                   | $7.86 \times 10^{-14}$ |
| cg07145664 | 6:2579591               |   |                     | 0.6933                         | 0.5966                              | 1.16                                   | $1.21 \times 10^{-13}$ |
| cg26968433 | 12:76397292             |   |                     | 0.7965                         | 0.7363                              | 1.08                                   | $1.28 \times 10^{-13}$ |
| cg24082440 | 21:33672186             | <i>MRAP</i>   | Body                | 0.8245                         | 0.7598                              | 1.09                                   | $1.53 \times 10^{-13}$ |
| cg27554156 | 12:13248725             | <i>GSG1</i>   | Body, TSS200        | 0.8345                         | 0.7781                              | 1.07                                   | $1.64 \times 10^{-13}$ |
| cg12433228 | 2:177486421             |   |                     | 0.6642                         | 0.5898                              | 1.13                                   | $1.83 \times 10^{-13}$ |
| cg12336358 | 1:114000078             | <i>MAGI3</i>  | Body                | 0.7586                         | 0.6597                              | 1.15                                   | $2.34 \times 10^{-13}$ |
| cg09723384 | 9:122217063             |   |                     | 0.5751                         | 0.6710                              | 0.86                                   | $2.89 \times 10^{-13}$ |
| cg05454595 | 5:139243335             | <i>NRG2</i>   | Body                | 0.6737                         | 0.5909                              | 1.14                                   | $5.69 \times 10^{-13}$ |
| cg06019613 | 2:18717524              |   |                     | 0.4711                         | 0.6044                              | 0.78                                   | $7.60 \times 10^{-13}$ |
| cg22651416 | 8:10643634              | <i>PINX1</i>  | Body                | 0.8567                         | 0.7935                              | 1.08                                   | $8.42 \times 10^{-13}$ |
| cg17882587 | 2:18933408              |   |                     | 0.6727                         | 0.5779                              | 1.16                                   | $8.56 \times 10^{-13}$ |
| cg19691778 | 8:97157756              | <i>GDF6</i>   | Body                | 0.3900                         | 0.5395                              | 0.72                                   | $9.03 \times 10^{-13}$ |
| cg17820365 | 8:97157856              | <i>GDF6</i>   | Body                | 0.2811                         | 0.4348                              | 0.65                                   | $9.07 \times 10^{-13}$ |
| cg15086256 | 2:222631916             |   |                     | 0.7039                         | 0.6146                              | 1.15                                   | $9.39 \times 10^{-13}$ |
| cg18141318 | 13:96350690             | <i>DNAJC3</i>   | Body                | 0.8180                         | 0.7723                              | 1.06                                   | $9.67 \times 10^{-13}$ |
| cg01754709 | 16:84961336             |   |                     | 0.7191                         | 0.6133                              | 1.17                                   | $9.74 \times 10^{-13}$ |
| cg17128320 | 4:78633646              |   |                     | 0.8804                         | 0.8235                              | 1.07                                   | $1.14 \times 10^{-12}$ |
| cg16597993 | 19:16578633             | <i>EPS15L1</i>  | Body                | 0.8226                         | 0.7540                              | 1.09                                   | $1.20 \times 10^{-12}$ |
| cg10224937 | 7:27208594              | <i>HOXA10-AS</i> ,<br><i>HOXA10</i> ,<br><i>HOXA9</i> | Body                | 0.5089                         | 0.6669                              | 0.76                                   | $1.32 \times 10^{-12}$ |
| cg12786452 | 17:62309293             | <i>TEX2</i>   | 5'UTR               | 0.8392                         | 0.7737                              | 1.08                                   | $1.44 \times 10^{-12}$ |
| cg05069228 | 3:61793623              | <i>PTPRG</i>  | Body                | 0.7403                         | 0.6545                              | 1.13                                   | $1.48 \times 10^{-12}$ |
| cg17741799 | 8:885656                |   |                     | 0.7770                         | 0.7158                              | 1.09                                   | $1.49 \times 10^{-12}$ |
| cg23854860 | 7:27208590              | <i>HOXA10-AS</i> ,<br><i>HOXA10</i> ,<br><i>HOXA9</i> | Body                | 0.5480                         | 0.6949                              | 0.79                                   | $1.67 \times 10^{-12}$ |
| cg03735712 | 15:35263065             | <i>AQR</i>  | TSS1500             | 0.7572                         | 0.6263                              | 1.21                                   | $1.69 \times 10^{-12}$ |
| cg09164580 | 8:97157878              | <i>GDF6</i>   | Body                | 0.4534                         | 0.6044                              | 0.75                                   | $1.73 \times 10^{-12}$ |
| cg10166915 | 14:54260975             |   |                     | 0.7714                         | 0.6711                              | 1.15                                   | $1.73 \times 10^{-12}$ |
| cg17868595 | 3:90112204              |   |                     | 0.7352                         | 0.8183                              | 0.90                                   | $1.74 \times 10^{-12}$ |
| cg00246590 | 12:126968300            |   |                     | 0.8422                         | 0.6984                              | 1.21                                   | $1.84 \times 10^{-12}$ |
| cg19183743 | 7:27188020              | <i>HOXA6</i>  | TSS1500             | 0.3144                         | 0.4401                              | 0.71                                   | $1.86 \times 10^{-12}$ |
| cg27584713 | 6:12717016              | <i>PHACTR1</i>  | TSS1500             | 0.6815                         | 0.5733                              | 1.19                                   | $1.98 \times 10^{-12}$ |
| cg02750391 | 11:14274978             | <i>SPON1</i>  | Body                | 0.7800                         | 0.7205                              | 1.08                                   | $2.04 \times 10^{-12}$ |
| cg21310745 | 7:27208454              | <i>HOXA10-AS</i> ,<br><i>HOXA10</i> ,<br><i>HOXA9</i> | TSS200, body        | 0.6244                         | 0.7815                              | 0.80                                   | $2.22 \times 10^{-12}$ |
| cg16739092 | 20:17519424             | <i>BFSP1</i>  | Body, 5'UTR         | 0.3781                         | 0.4932                              | 0.77                                   | $2.23 \times 10^{-12}$ |
| cg03804397 | 11:76925617             | <i>MYO7A</i>  | Body                | 0.7302                         | 0.6427                              | 1.14                                   | $2.31 \times 10^{-12}$ |
| cg22790931 | 7:39017455              | <i>POU6F2</i>   | TSS200              | 0.9070                         | 0.8683                              | 1.04                                   | $2.36 \times 10^{-12}$ |



Table II. Continued.

| CpG        | Chromosome:<br>position | Gene           | Methylation<br>site | Mean $\beta$ value<br>(plaque) | Mean $\beta$ value<br>(plaque-free) | $\beta$ ratio (plaque/<br>plaque-free) | P-value                |
|------------|-------------------------|----------------|---------------------|--------------------------------|-------------------------------------|--|------------------------|
| cg23080761 | 12:111857575            | <i>SH2B3</i>   | Body                | 0.8194                         | 0.7611                              | 1.08                                   | $3.04 \times 10^{-12}$ |
| cg13913011 | 9:132711808             | <i>FNBP1</i>   | Body                | 0.7628                         | 0.6517                              | 1.17                                   | $3.18 \times 10^{-12}$ |
| cg08272913 | 18:68079266             |                |                     | 0.6156                         | 0.4664                              | 1.32                                   | $3.33 \times 10^{-12}$ |
| cg20337028 | 17:75181836             | <i>SEC14L1</i> | Body, 5'UTR         | 0.7624                         | 0.6871                              | 1.11                                   | $3.44 \times 10^{-12}$ |
| cg12873661 | 1:166277235             |                |                     | 0.6713                         | 0.5187                              | 1.29                                   | $3.48 \times 10^{-12}$ |

TSS1500 (200), within 1,500 (200) bp from the transcription start site;  $P < 5.86 \times 10^{-8}$  was considered statistically significant. NRG2, neuregulin 2; SPRY2, sprout RTK signaling antagonist 2; PCDHGA8, protocadherin gamma subfamily A8; AOAH, acyloxyacyl hydrolase; OCA2, oculocutaneous albinism type 2; HOXA9, homeobox A9; PHACTR1, phosphatase actin regulator 1; MRAP, melanocortin 2 receptor accessory protein; GSG1, germ cell associated 1; MAGI3, membrane associated guanylate kinase, WW and PD2 domains-containing 3; PINX1, PIN2/TERF1 interacting telomerase inhibitor 1; GDF6, growth differentiation factor 6; DNAJC3, DnaJ heat shock protein family member C3; EPS1SL1, epidermal growth factor receptor pathway substrate 13-like; AS, antisense RNA; TEX2, testis expressed 2; PTPRG, protein tyrosine phosphatase receptor type G; AQR, Aquarius intron-binding splicing factor; SPON1, spondin 1; BFSP1, beaded filament structural protein 1; MYO7A, myosin VIIa; SH2B3, SH2B adaptor protein 3; FNBP1, formin binding protein 1; SEC14L1, SEC14-like lipid binding 1; TSS, transcription start site; UTR, untranslated region.

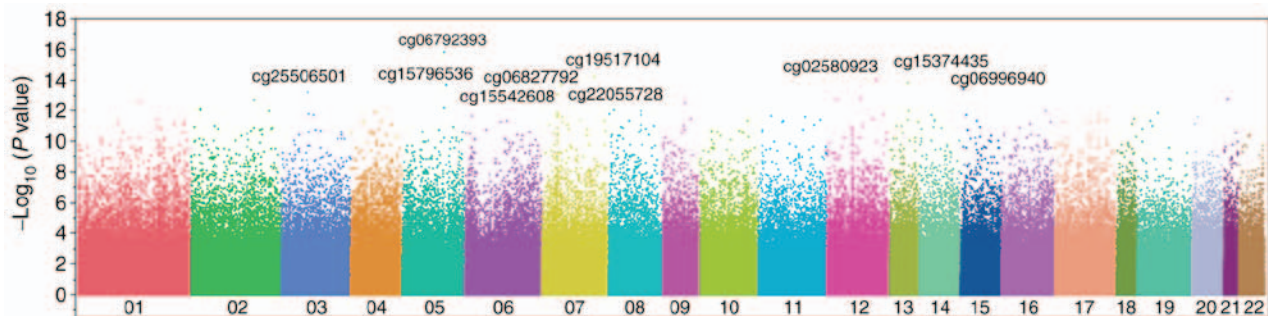


Figure 1. Manhattan plot of P-values in the genome-wide analysis of CpG site methylation differences between atheromatous plaque and plaque-free intima. P-values (y-axis) are plotted as  $-\log_{10}(P)$  with respect to the physical chromosomal positions of the corresponding CpG sites (x-axis). The 10 CpG sites with the lowest P-values are indicated.

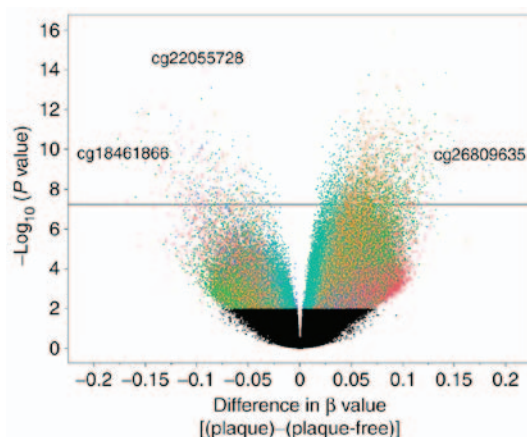


Figure 2. Volcano plot for the genome-wide analysis of differences in CpG site methylation between atheromatous plaques and plaque-free intimas. The x- and y-axes represent the difference in  $\beta$  values and P-values as  $-\log_{10}(P)$ , respectively. The right and left halves of the plot correspond to hyper- or hypomethylation, respectively, in atheromatous plaque lesions compared with plaque-free intima. The significance threshold is indicated by the horizontal line. The CpG site cg26809635, which was hypermethylated in plaque lesions, had the largest difference in  $\beta$  value (0.1834) and the largest  $\beta$  ratio (3.20) and is indicated on the plot. The CpG sites hypomethylated in plaque lesions with the largest difference in  $\beta$  values (-0.1799, cg18461866) or the smallest  $\beta$  ratio (0.57, cg22055728) are also marked presented.

## Discussion

Atherosclerosis occurs as a result of endothelial damage and dysfunction that leads to the accumulation and oxidation of low-density lipoprotein (LDL) cholesterol in the vessel wall. Monocytes migrate from blood into the subendothelial intima and transform into macrophages, which accumulate lipids as foam cells in the lipid core of the atherosclerotic plaque (26,27). Inflammatory and thrombotic processes serve primary roles in the formation of atherosclerotic lesions and subsequent plaque rupture that causes acute coronary syndrome (26,27). A number of mechanisms by which changes in DNA methylation may affect the development of atherosclerosis have been identified. These mechanisms include the promotion of inflammation, endothelial dysfunction, proliferation and migration of smooth muscle cells or monocyte-macrophages, extracellular matrix production, homocysteine metabolism and apoptosis of vascular cells (12,28,29). However, given the dynamic nature and tissue heterogeneity of atherosclerosis, defining the precise role of DNA methylation in the pathogenesis of this condition is challenging (12). A marked increase in DNA methylation in atherosclerotic lesions may warrant the development of DNA demethylation agents, including DNA methyltransferase

Table III. Five CpG sites whose methylation status differed significantly ( $P < 5.86 \times 10^{-8}$ ) between atheromatous plaque lesions and plaque-free intima with a difference in  $\beta$  values (plaque lesion-plaque-free intima) of  $>0.15$ .

| CpG        | Chromosome:<br>position | Gene         | Mean $\beta$ value<br>(plaque) | Mean $\beta$ value<br>(plaque-free) | $\beta$ ratio (plaque/<br>plaque-free) | Difference in $\beta$ values<br>(plaque-plaque-free) | P-value                |
|------------|-------------------------|--------------|--------------------------------|-------------------------------------|--|--|------------------------|
| cg26809635 | 12:54355087             |              | 0.2669                         | 0.0835                              | 3.1957                                 | 0.1834   | $6.35 \times 10^{-10}$ |
| cg23786812 | 7:156296516             |              | 0.5526                         | 0.3922                              | 1.4090                                 | 0.1604   | $4.12 \times 10^{-12}$ |
| cg15648389 | 12:54448769             | <i>HOXC4</i> | 0.5564                         | 0.4005                              | 1.3893                                 | 0.1559   | $3.60 \times 10^{-11}$ |
| cg27178293 | 12:54371246             |              | 0.4042                         | 0.2484                              | 1.6270                                 | 0.1558   | $1.24 \times 10^{-8}$  |
| cg12873661 | 1:166277235             |              | 0.6713                         | 0.5187                              | 1.2941                                 | 0.1526   | $3.48 \times 10^{-12}$ |

*HOXC4*, homeobox C4.

Table IV. Eleven CpG sites whose methylation status differed significantly ( $P < 5.86 \times 10^{-8}$ ) between atheromatous plaque lesions and plaque-free intima with a  $\beta$  ratio (plaque/plaque-free) of  $>1.50$ .

| CpG        | Chromosome:<br>position | Gene                     | Methylation<br>site | Mean $\beta$ value<br>(plaque) | Mean $\beta$ value<br>(plaque-free) | $\beta$ ratio (plaque/<br>plaque-free) | P-value                |
|------------|-------------------------|--------------------------|---------------------|--------------------------------|-------------------------------------|--|------------------------|
| cg26809635 | 12:54355087             |                          |                     | 0.2669                         | 0.0835                              | 3.20                                   | $6.35 \times 10^{-10}$ |
| cg18040901 | 12:54357530             | <i>HOTAIR</i>            | Body                | 0.1839                         | 0.0979                              | 1.88                                   | $6.12 \times 10^{-11}$ |
| cg00576279 | 12:54427293             | <i>HOXC4, HOXC5</i>      | 5'UTR, body         | 0.2516                         | 0.1419                              | 1.77                                   | $5.04 \times 10^{-9}$  |
| cg17466857 | 7:27225528              | <i>HOXA11-AS, HOXA11</i> | Body, TSS1500       | 0.2618                         | 0.1479                              | 1.77                                   | $1.16 \times 10^{-8}$  |
| cg08857479 | 12:54369987             | <i>HOXC11</i>            | 3'UTR               | 0.3479                         | 0.2112                              | 1.65                                   | $1.93 \times 10^{-8}$  |
| cg27178293 | 12:54371246             |                          |                     | 0.4042                         | 0.2484                              | 1.63                                   | $1.24 \times 10^{-8}$  |
| cg15700739 | 12:54427700             | <i>HOXC4, HOXC5</i>      | 5'UTR, body         | 0.3313                         | 0.2050                              | 1.62                                   | $1.15 \times 10^{-9}$  |
| cg00862376 | 12:54343711             |                          |                     | 0.2745                         | 0.1708                              | 1.61                                   | $5.27 \times 10^{-9}$  |
| cg00187380 | 12:54427384             | <i>HOXC4, HOXC5</i>      | 5'UTR, body         | 0.3373                         | 0.2144                              | 1.57                                   | $2.21 \times 10^{-8}$  |
| cg02384661 | 12:54369638             | <i>HOXC11</i>            | 3'UTR               | 0.3804                         | 0.2450                              | 1.55                                   | $5.36 \times 10^{-9}$  |
| cg05951084 | 12:54343681             |                          |                     | 0.3480                         | 0.2304                              | 1.51                                   | $7.64 \times 10^{-9}$  |

TSS1500, within 1,500 bp from the transcription start site. *HOTAIR*, *HOX* transcript antisense RNA; *HOX*, homeobox; -AS, antisense RNA; UTR, untranslated region; TSS, transcription start site.

inhibitors, for the treatment of atherosclerotic cardiovascular disease (29).

Arteriosclerosis is classified into three types: atherosclerosis, Mönckeberg medial sclerosis and arteriolosclerosis (30). Given that atherosclerosis is the most important pathological change in the development of cardiovascular disease (1,26,27,30), the aortic intima was examined in the present study. The results revealed that 2,272 and 407 CpG sites were hyper- and hypomethylated, respectively, in genomic DNA isolated from atheromatous plaque lesions compared with matched plaque-free intima. A total of 5 CpG sites had a  $>0.15$  difference in  $\beta$  values and 11 CpG sites had a  $\beta$  ratio of  $>1.50$ . Among these CpG sites, cg15648389 of *HOXC4* (15), cg17466857 of *HOXA11-HOXA11-AS* (14,15), cg15700739 of *HOXC4/HOXC5* (17) and cg02384661 of *HOXC11* (15) have previously been reported to be associated with atherosclerosis. A total of 10 novel CpG sites (cg26809635, cg23786812, cg27178293, cg12873661, cg18040901, cg00576279,

cg08857479, cg00862376, cg00187380, cg05951084) that were significantly hypermethylated in atheromatous plaque lesions compared with plaque-free intima were identified in the present study. Of these 10 CpG sites, cg18040901 is located in the *HOX transcript antisense RNA (HOTAIR)* gene, whose methylation status has not previously been associated with atherosclerosis. The *HOTAIR* gene is located at chromosome 12q13.13 and encodes a protein that has been reported to promote the proliferation and migration of vascular endothelial cells and to protect these cells against oxidized LDL-induced injury and apoptosis (31). Endothelial damage and dysfunction are early key processes in the development of atherosclerosis, resulting in the accumulation and oxidation of LDL-cholesterol in the arterial wall (26,27), and so *HOTAIR* may protect against this (31).

A total of 15 CpG sites with a  $<0.15$  difference in  $\beta$  values and 17 CpG sites with a  $\beta$  ratio of  $<0.67$  were identified in the present study, including 2 CpG sites (cg13669152,

Table V. Fifteen CpG sites whose methylation status differed significantly ( $P < 5.86 \times 10^{-8}$ ) between atheromatous plaque lesions and plaque-free intima with a difference in  $\beta$  values (plaque lesion-plaque-free intima) of  $< -0.15$ .

| CpG        | Chromosome:<br>position | Gene   | Mean $\beta$ value<br>(plaque) | Mean $\beta$ value<br>(plaque-free) | $\beta$ ratio<br>(plaque/<br>plaque-free) | Difference in<br>$\beta$ values<br>(plaque-plaque-free) | P-value                |
|------------|-------------------------|--|--------------------------------|-------------------------------------|---|---|------------------------|
| cg18461866 | 3:59996864              | <i>FHIT</i>  | 0.3759                         | 0.5558                              | 0.6763                                    | -0.1799   | $1.78 \times 10^{-10}$ |
| cg21007852 | 7:27203546              | <i>HOXA9</i>                                       | 0.5134                         | 0.6904                              | 0.7435                                    | -0.1771   | $2.96 \times 10^{-11}$ |
| cg25227803 | 10:102239027            | <i>WNT8B</i>                                       | 0.3980                         | 0.5727                              | 0.6951                                    | -0.1746   | $1.84 \times 10^{-11}$ |
| cg03217995 | 7:27203430              | <i>HOXA9</i>                                       | 0.5377                         | 0.7107                              | 0.7565                                    | -0.1731   | $5.49 \times 10^{-10}$ |
| cg02886033 | 7:27208114              |  | 0.5367                         | 0.7048                              | 0.7615                                    | -0.1681   | $7.82 \times 10^{-10}$ |
| cg11052578 | 21:39695801             |  | 0.3391                         | 0.5064                              | 0.6697                                    | -0.1672   | $4.05 \times 10^{-8}$  |
| cg13669152 | 6:130923610             |  | 0.4987                         | 0.6580                              | 0.7579                                    | -0.1593   | $2.46 \times 10^{-8}$  |
| cg10224937 | 7:27208594              | <i>HOXA10-AS</i> ,<br><i>HOXA10</i> , <i>HOXA9</i> | 0.5089                         | 0.6669                              | 0.7631                                    | -0.1580   | $1.32 \times 10^{-12}$ |
| cg09699744 | 12:54390705             | <i>HOXC-AS2</i>                                    | 0.3719                         | 0.5298                              | 0.7020                                    | -0.1579   | $1.60 \times 10^{-10}$ |
| cg21310745 | 7:27208454              | <i>HOXA10-AS</i> ,<br><i>HOXA10</i> , <i>HOXA9</i> | 0.6244                         | 0.7815                              | 0.7990                                    | -0.1571   | $2.22 \times 10^{-12}$ |
| cg01016793 | 15:64894722             | <i>ZNF609</i>                                      | 0.4212                         | 0.5773                              | 0.7297                                    | -0.1561   | $1.03 \times 10^{-11}$ |
| cg10374314 | 7:27189610              | <i>HOXA-AS3</i>                                    | 0.5017                         | 0.6558                              | 0.7650                                    | -0.1541   | $4.03 \times 10^{-11}$ |
| cg17820365 | 8:97157856              | <i>GDF6</i>  | 0.2811                         | 0.4348                              | 0.6465                                    | -0.1537   | $9.07 \times 10^{-13}$ |
| cg09164580 | 8:97157878              | <i>GDF6</i>  | 0.4534                         | 0.6044                              | 0.7502                                    | -0.1510   | $1.73 \times 10^{-12}$ |
| cg06136628 | 7:35289993              | <i>TBX20</i>                                       | 0.2790                         | 0.4293                              | 0.6498                                    | -0.1503   | $4.81 \times 10^{-10}$ |

FHIT, fragile histidine triad; HOX, homeobox; WNT8B, wnt family member 8B; -AS, antisense RNA; ZNF609, zinc finger protein 609; GDF6, growth differentiation factor 6; TBX20, T-box 20.

Table VI. Seventeen CpG sites whose methylation status differed significantly ( $P < 5.86 \times 10^{-8}$ ) between atheromatous plaque lesions and plaque-free intima with a  $\beta$  ratio (plaque/plaque-free) of  $< 0.67$ .

| CpG        | Chromosome:<br>position | Gene                             | Methylation<br>site | Mean $\beta$ value<br>(plaque) | Mean $\beta$ value<br>(plaque-free) | $\beta$ ratio<br>(plaque/plaque-free) | P-value                |
|------------|-------------------------|----------------------------------|---------------------|--------------------------------|-------------------------------------|---------------------------------------|------------------------|
| cg22055728 | 7:27205658              | <i>HOXA9</i>                     | TSS1500             | 0.1162                         | 0.2026                              | 0.57                                  | $7.80 \times 10^{-14}$ |
| cg13335081 | 8:66894111              |                                  |                     | 0.1758                         | 0.2913                              | 0.60                                  | $1.67 \times 10^{-8}$  |
| cg23345300 | 2:177000621             |                                  |                     | 0.1669                         | 0.2752                              | 0.61                                  | $3.81 \times 10^{-8}$  |
| cg04122553 | 14:21250646             |                                  |                     | 0.1587                         | 0.2615                              | 0.61                                  | $3.43 \times 10^{-9}$  |
| cg24719020 | 7:27187943              | <i>HOXA6</i>                     | TSS1500             | 0.2018                         | 0.3324                              | 0.61                                  | $1.51 \times 10^{-9}$  |
| cg14554869 | 5:74231171              |                                  |                     | 0.1656                         | 0.2630                              | 0.63                                  | $9.29 \times 10^{-11}$ |
| cg11348442 | 2:220117784             | <i>TUBA4B</i> ,<br><i>TUBA4A</i> | TSS200, body        | 0.1177                         | 0.1869                              | 0.63                                  | $5.22 \times 10^{-8}$  |
| cg10893095 | 6:85478296              |                                  |                     | 0.2545                         | 0.4008                              | 0.64                                  | $1.10 \times 10^{-10}$ |
| cg26437522 | 7:27174169              |                                  |                     | 0.2220                         | 0.3460                              | 0.64                                  | $4.59 \times 10^{-9}$  |
| cg01428378 | 12:123259789            | <i>CCDC62</i>                    | Body                | 0.1784                         | 0.2770                              | 0.64                                  | $2.67 \times 10^{-8}$  |
| cg17820365 | 8:97157856              | <i>GDF6</i>                      | Body                | 0.2811                         | 0.4348                              | 0.65                                  | $9.07 \times 10^{-13}$ |
| cg25541958 | 8:1992965               | <i>MYOM2</i>                     | TSS200              | 0.1679                         | 0.2585                              | 0.65                                  | $4.63 \times 10^{-11}$ |
| cg06136628 | 7:35289993              | <i>TBX20</i>                     | Body                | 0.2790                         | 0.4293                              | 0.65                                  | $4.81 \times 10^{-10}$ |
| cg19783626 | 7:98311436              |                                  |                     | 0.2204                         | 0.3366                              | 0.65                                  | $3.72 \times 10^{-12}$ |
| cg00980698 | 14:21250509             | <i>RNASE6</i>                    | 3'UTR               | 0.1554                         | 0.2365                              | 0.66                                  | $1.67 \times 10^{-10}$ |
| cg12110087 | 7:27187691              | <i>HOXA6</i>                     | TSS1500             | 0.2103                         | 0.3168                              | 0.66                                  | $8.08 \times 10^{-9}$  |
| cg11052578 | 21:39695801             |                                  |                     | 0.3391                         | 0.5064                              | 0.66                                  | $4.05 \times 10^{-8}$  |

TSS1500 (200), within 1,500 (200) bp from the transcription start site. HOX, homeobox; TUBA4B/4A, tubulin alpha 4a and 4b; CCDC62, coiled-coil domain containing 62; GDF6, growth differentiation factor 6; MYOM2, myomesin 2; TBX2-, T-box 20; RNASE6, ribonuclease A family member k6; TSS, transcription start site; UTR, untranslated region.



cg13335081) located in enhancer regions as described by the FANTOM5 project (24). Of these sites, cg03217995 of *HOXA9* (15) was previously reported to be associated with atherosclerosis. Additionally, 28 novel CpG sites that were significantly hypomethylated in atheromatous plaque lesions compared with plaque-free intima were identified in the present study: cg18461866, cg21007852, cg25227803, cg02886033, cg11052578, cg13669152, cg10224937, cg09699744, cg21310745, cg01016793, cg10374314, cg17820365, cg09164580, cg06136628, cg22055728, cg13335081, cg23345300, cg04122553, cg24719020, cg14554869, cg11348442, cg10893095, cg26437522, cg01428378, cg25541958, cg19783626, cg00980698 and cg12110087. Of these sites, 16 are located in genes whose methylation status has not previously been reported as associated with atherosclerosis, including *fragile histidine triad* (*FHIT*; cg18461866), *wnt family member 8B* (*WNT8B*; cg25227803), *HOXA10-HOXA10-antisense RNA* (*AS*; cg10224937 and cg21310745), *HOXC cluster antisense RNA 2* (*HOXC-AS2*; cg09699744), *zinc finger protein 609* (*ZNF609*; cg01016793), *HOXA-AS3* (cg10374314), *growth differentiation factor 6* (*GDF6*; cg17820365, cg09164580), *T-box 20* (*TBX20*; cg06136628), *HOXA6* (cg24719020, cg12110087), *tubulin alpha 4a and 4b* (*TUBA4A/TUBA4B*; cg11348442), *coiled-coil domain containing 62* (*CCDC62*; cg01428378), *myomesin 2* (*MYOM2*; cg25541958) and *ribonuclease A family member k6* (*RNASE6*; cg00980698).

*TBX20* is located at chromosome 7p14.2 and encodes a protein that has been demonstrated to protect endothelial cells against oxidized LDL-induced injury via upregulating peroxisome proliferator-activated receptor  $\gamma$ , indicating that it may protect against the development of atherosclerosis (32). It has also previously been determined that a polymorphism (rs3206736) near *TBX20* is associated with a decrease in diastolic blood pressure (33). Several of the genes that were demonstrated to be hypomethylated in atherosclerotic tissues in the present study have been reported to be correlated with atherosclerosis-related phenotypes: The *FHIT* gene located at chromosome 3p14.2 is associated with body mass index (34); the *HOXA10-HOXA10-AS* gene at 7p15.2 is expressed differentially in porcine coronary and iliac artery endothelial cells (35); the *HOXA-AS3* gene at 7p15.2 is associated with chronic venous disease (36) and monocyte count (37); *HOXA6* at 7p15.2 is associated with chronic venous disease (36); and the *TUBA4A/TUBA4B* gene at 2q35 is associated with the size distribution of platelets (37). The remaining novel genes identified in the present study (*WNT8B* located at chromosome 10q24.31; *HOXC-AS2* at 12q13.13; *ZNF609* at 15q22.31; *GDF6* at 8q22.1; *CCDC62* at 12q24.31; *MYOM2* at 8p23.3; and the *RNASE6* gene at 14q11.2) have not previously been reported as associated with atherosclerosis-related phenotypes.

It was previously demonstrated that the methylation at 45 CpG sites differed significantly ( $P < 1.03 \times 10^{-7}$ ) between atheromatous plaque lesions and plaque-free intima (19). The associations between 23 of these CpG sites [cg02240539 ( $P = 0.0499$ ), cg04304054 ( $P = 0.0071$ ), cg14521421 ( $P = 0.0033$ ), cg14477581 ( $P = 0.0302$ ), cg00909706 ( $P = 3.49 \times 10^{-6}$ ), cg00716848 ( $P = 0.0009$ ), cg08466030 ( $P = 8.08 \times 10^{-6}$ ), cg22046201 ( $P = 0.0002$ ), cg18516609 ( $P = 0.0188$ ), cg24634746 ( $P = 8.43 \times 10^{-6}$ ), cg26619894 ( $P = 1.20 \times 10^{-5}$ ), cg03962451

( $P = 5.52 \times 10^{-5}$ ), cg12556802 ( $P = 4.90 \times 10^{-7}$ ), cg10586883 ( $P = 0.0309$ ), cg06208382 ( $P = 1.06 \times 10^{-6}$ ), cg18177814 ( $P = 0.0013$ ), cg20556639 ( $P = 1.07 \times 10^{-6}$ ), cg09349128 ( $P = 0.0112$ ), cg26724841 ( $P = 0.0379$ ), cg02196592 ( $P = 0.0235$ ), cg16906765 ( $P = 0.0032$ ), cg27647755 ( $P = 1.16 \times 10^{-6}$ ), cg01473038 ( $P = 0.0044$ )] to atherosclerosis were replicated in the present study.

There are several limitations to the present study: i) The aortic intima specimens comprised heterogeneous cell types, as described previously (19). ii) Although DNA methylation status may differ among atherosclerosis, Mönckeberg medial sclerosis and arteriolosclerosis, only the aortic intima was examined. iii) The association between atherosclerosis grade and DNA methylation status was not assessed. iv) The effects of hyper- or hypomethylation of CpG sites on the expression of genes were not investigated. v) Given the small sample size of the current study, the statistical power of the genome-wide analysis of DNA methylation was not optimal. vi) The molecular mechanisms underlying the effects of DNA methylation identified in the present study have not been determined definitively. vii) The validation of the results of the present study will require replication with other independent subject panels.

In conclusion, 16 novel genes that were significantly hyper- or hypomethylated in atheromatous plaque lesions compared with plaque-free intima were identified in the present study. These results suggest that the methylation status of these genes may contribute to the pathogenesis of atherosclerosis. The determination of DNA methylation status for the identified CpG sites may prove informative for the assessment of epigenetic risks associated with atherosclerotic cardiovascular disease in the Japanese population.

## Acknowledgements

The present study was supported by CREST (grant no. JPMJCR1302), Japan Science and Technology Agency (Kawaguchi, Japan).

## Competing interests

The authors declare that they have no competing interests.

## References

1. Lusis AJ: Atherosclerosis. *Nature* 407: 233-241, 2000.
2. Baccarelli A, Rienstra M and Benjamin EJ: Cardiovascular epigenetics: Basic concepts and results from animal and human studies. *Circ Cardiovasc Genet* 3: 567-573, 2010.
3. Neele AE, Van den Bossche J, Hoeksema MA and de Winther MP: Epigenetic pathways in macrophages emerge as novel targets in atherosclerosis. *Eur J Pharmacol* 763: 79-89, 2015.
4. Rakyan VK, Down TA, Balding DJ and Beck S: Epigenome-wide association studies for common human diseases. *Nat Rev Genet* 12: 529-541, 2011.
5. Handy DE, Castro R and Loscalzo J: Epigenetic modifications: Basic mechanisms and role in cardiovascular disease. *Circulation* 123: 2145-2156, 2011.
6. Tsai PC, Spector TD and Bell JT: Using epigenome-wide association scans of DNA methylation in age-related complex human traits. *Epigenomics* 4: 511-526, 2012.
7. Pfeiffer L, Wahl S, Pilling LC, Reischl E, Sandling JK, Kunze S, Holdt LM, Kretschmer A, Schramm K, Adamski J, *et al*: DNA methylation of lipid-related genes affects blood lipid levels. *Circ Cardiovasc Genet* 8: 334-342, 2015.



8. Rask-Andersen M, Martinsson D, Ahsan M, Enroth S, Ek WE, Gyllenstein U and Johansson Å: Epigenome-wide association study reveals differential DNA methylation in individuals with a history of myocardial infarction. *Hum Mol Genet* 25: 4739-4748, 2016.
9. Wahl S, Drong A, Lehne B, Loh M, Scott WR, Kunze S, Tsai PC, Ried JS, Zhang W, Yang Y, *et al*: Epigenome-wide association study of body mass index, and the adverse outcomes of adiposity. *Nature* 541: 81-86, 2017.
10. Li J, Zhu X, Yu K, Jiang H, Zhang Y, Deng S, Cheng L, Liu X, Zhong J, Zhang X, *et al*: Genome-wide analysis of DNA methylation and acute coronary syndrome. *Circ Res* 120: 1754-1767, 2017.
11. Fernández-Sanlés A, Sayols-Baixeras S, Subirana I, Degano IR and Elosua R: Association between DNA methylation and coronary heart disease or other atherosclerotic events: A systematic review. *Atherosclerosis* 263: 325-333, 2017.
12. Khyzha N, Alizada A, Wilson MD and Fish JE: Epigenetics of atherosclerosis: Emerging mechanisms and methods. *Trends Mol Med* 23: 332-347, 2017.
13. Deaton AM and Bird A: CpG islands and the regulation of transcription. *Genes Dev* 25: 1010-1022, 2011.
14. Nazarenko MS, Puzyreva VP, Lebedev IN, Frolov AV, Barbarash OL and Barbarash LS: Methylation profiling of DNA in the area of atherosclerotic plaque in humans. *Mol Biol* 45: 561, 2011.
15. Zaina S, Heyn H, Carmona FJ, Varol N, Sayols S, Condom E, Ramírez-Ruz J, Gomez A, Gonçalves I, Moran S and Esteller M: DNA methylation map of human atherosclerosis. *Circ Cardiovasc Genet* 7: 692-700, 2014.
16. Aavik E, Lumivuori H, Leppänen O, Wirth T, Häkkinen SK, Bräsen JH, Beschoner U, Zeller T, Braspenning M, van Criekinge W, *et al*: Global DNA methylation analysis of human atherosclerotic plaques reveals extensive genomic hypomethylation and reactivation at imprinted locus 14q32 involving induction of a miRNA cluster. *Eur Heart J* 36: 993-1000, 2015.
17. Kucher AN, Nazarenko MS, Markov AV, Koroleva IA and Barbarash OL: Variability of methylation profiles of CpG sites in microRNA genes in leukocytes and vascular tissues of patients with atherosclerosis. *Biochemistry* 82: 698-706, 2017.
18. Castillo-Díaz SA, Garay-Sevilla ME, Hernández-González MA, Solís-Martínez MO and Zaina S: Extensive demethylation of normally hypermethylated CpG islands occurs in human atherosclerotic arteries. *Int J Mol Med* 26: 691-700, 2010.
19. Yamada Y, Nishida T, Horibe H, Oguri M, Kato K and Sawabe M: Identification of hypo- and hypermethylated genes related to atherosclerosis by a genome-wide analysis of DNA methylation. *Int J Mol Med* 33: 1355-1363, 2014.
20. Moran S, Arribas C and Esteller M: Validation of a DNA methylation microarray for 850,000 CpG sites of the human genome enriched in enhancer sequences. *Epigenomics* 8: 389-399, 2016.
21. Christensen BC, Houseman EA, Marsit CJ, Zheng S, Wrensch MR, Wiemels JL, Nelson HH, Karagas MR, Padbury JF, Bueno R, *et al*: Aging and environmental exposures alter tissue-specific DNA methylation dependent upon CpG island context. *PLoS Genet* 5: e1000602, 2009.
22. Bell JT, Pai AA, Pickrell JK, Gaffney DJ, Pique-Regi R, Degner JF, Gilad Y and Pritchard JK: DNA methylation patterns associate with genetic and gene expression variation in HapMap cell lines. *Genome Biol* 12: R10, 2011.
23. ENCODE Project Consortium: An integrated encyclopedia of DNA elements in the human genome. *Nature* 489: 57-74, 2012.
24. Lizio M, Harshbarger J, Shimoji H, Severin J, Kasukawa T, Sahin S, Abugessaisa I, Fukuda S, Hori F, Ishikawa-Kato S, *et al*: Gateways to the FANTOM5 promoter level mammalian expression atlas. *Genome Biol* 16: 22, 2015.
25. Bibikova M, Barnes B, Tsan C, Ho V, Klotzle B, Le JM, Delano D, Zhang L, Schroth GP, Gunderson KL, *et al*: High density DNA methylation array with single CpG site resolution. *Genomics* 98: 288-295, 2011.
26. Libby P: Inflammation in atherosclerosis. *Nature* 420: 868-874, 2002.
27. Libby P: Mechanisms of acute coronary syndromes and their implications for therapy. *N Engl J Med* 368: 2004-2013, 2013.
28. Turunen MP, Aavik E and Ylä-Herttuala S: Epigenetics and atherosclerosis. *Biochim Biophys Acta* 1790: 886-891, 2009.
29. Hai Z and Zuo W: Aberrant DNA methylation in the pathogenesis of atherosclerosis. *Clin Chim Acta* 456: 69-74, 2016.
30. Fishbein GA and Fishbein MC: Arteriosclerosis: Rethinking the current classification. *Arch Pathol Lab Med* 133: 1309-1316, 2009.
31. Peng Y, Meng K, Jiang L, Zhong Y, Yang Y, Lan Y, Zeng Q and Cheng L: Thymic stromal lymphopoietin-induced HOTAIR activation promotes endothelial cell proliferation and migration in atherosclerosis. *Biosci Rep* 37: pii: BSR20170351, 2017.
32. Shen T, Zhu Y, Patel J, Ruan Y, Chen B, Zhao G, Cao Y, Pang J, Guo H, Li H, *et al*: T-box20 suppresses oxidized low-density lipoprotein-induced human vascular endothelial cell injury by upregulation of PPAR-γ. *Cell Physiol Biochem* 32: 1137-1150, 2013.
33. Warren HR, Evangelou E, Cabrera CP, Gao H, Ren M, Mifsud B, Ntalla I, Surendran P, Liu C, Cook JP, *et al*: Genome-wide association analysis identifies novel blood pressure loci and offers biological insights into cardiovascular risk. *Nat Genet* 49: 403-415, 2017.
34. Graff M, Scott RA, Justice AE, Young KL, Feitosa MF, Barata L, Winkler TW, Chu AY, Mahajan A, Hadley D, *et al*: Genome-wide physical activity interactions in adiposity-a meta-analysis of 200,452 adults. *PLoS Genet* 13: e1006528, 2017.
35. Zhang J, Burridge KA and Friedman MH: In vivo differences between endothelial transcriptional profiles of coronary and iliac arteries revealed by microarray analysis. *Am J Physiol Heart Circ Physiol* 295: H1556-H1561, 2008.
36. Ellinghaus E, Ellinghaus D, Krusche P, Greiner A, Schreiber C, Nikolaus S, Gieger C, Strauch K, Lieb W, Rosenstiel P, *et al*: Genome-wide association analysis for chronic venous disease identifies EFEMP1 and KCNH8 as susceptibility loci. *Sci Rep* 7: 45652, 2017.
37. Astle WJ, Elding H, Jiang T, Allen D, Ruklisa D, Mann AL, Mead D, Bouman H, Riveros-Mckay F, Kostadima MA, *et al*: The allelic landscape of human blood cell trait variation and links to common complex disease. *Cell* 167: 1415-1429.e19, 2016.



This work is licensed under a Creative Commons Attribution-NonCommercial-NoDerivatives 4.0 International (CC BY-NC-ND 4.0) License.